A Novel Three-Phase Oak Ridge AC / AC Converter for Wireless Mobility Energy Storage System (WMESS) Connectivity

Erdem Asa, Omer C. Onar, Veda P. Galigekere, Gui-Jia Su, and Burak Ozpineci
Buildings and Transportation Science Division, Oak Ridge National Laboratory
National Transportation Research Center, Knoxville, TN 37932, USA
E-mail: asae@ornl.com

***Abstract*— In this study, a novel three-phase Oak Ridge ac to ac converter is introduced for wireless mobility energy storage system (WMESS) applications for grid support or ancillary service applications. The proposed topology can be used in bidirectional operation between ac grid and ac terminals of energy storage (output of the ESS inverter) by accomplishing unity power factor. Inherent merit of the technology is that it can directly merge ac input 60 Hz grid frequency with the high frequency by superimposing them with the Oak Ridge Converter (ORC) and through the wireless coils. Theoretical and simulation results are provided for 10 kW output power. The functionality of the proposed three-phase system is demonstrated with the coupling coils separated by 6 inches of air gap with the input / output of 277 $V_{AC,RMS}$. The system overall design is presented, and simulation results demonstrate achieving 3% current total harmonic distortion (THD) and 0.99 power factor (PF) at full load of 10 kW wireless power transfer.**

Keywords*— *Oak Ridge, resonant, converter, grid, high frequency, wireless, bi-directional, grid support, mobile, ESS

I. INTRODUCTION

Due to their very fast response times, ESSs can be used for several applications from grid support services to renewable energy firming and transportation applications [1]-[2]. Combining ESSs with renewable energy sources is one of the most appealing methods to improve renewable energy integration with compensated intermittencies and reduced fluctuations [3]-[4]. ESSs can also be used to provide grid support and grid ancillary services [2]. Considerable amount of ESSs are required with the increasing number of solar and wind farms to provide grid reliability and stability including grid network delays, reactive power support, peak shaving, time of use energy cost management, spinning or contingency reserves, area or frequency regulation, transmission, or distribution equipment upgrade deferral, etc. However, unpredictable output variation and uncertain energy fluctuations of renewable sources might impact to the grid operations if ESSs are not properly managed. Integrated microgrid systems are proposed with mobility ESSs to solve the mentioned complications in the literature [5]-[6]. Wireless power transfer (WPT) has several advantages compared to wired power systems, especially for mobile ESSs [7]-[8]. During power outages or peak load time, mobile ESSs becomes an extremely critical aspect of deploying power to the affected sites. WPT-based connectivity provides easy deployment, connection, reconfiguration, and relocation of the ESS systems. It is more difficult to deploy the wired systems as they get bulky as the power increases. They may require a special type of connector or a plug system that may not be available on the site at the time of deployment. WPT technology offers flexible and rapid deployment and provides inherent galvanic isolation which are the two critical components for use in harsh environments and inclement weather conditions for emergency power systems. With the elimination of physical electrical contacts, bidirectional WPT is an attractive solution for the back-and-forth energy transfer between grid and ESSs [9]-[10].

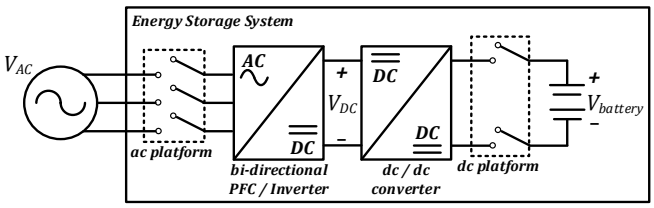

Fig. 1. A conventional energy storage system, ac and dc platforms with integrated on-board bidirectional ac / dc and dc / dc conversions.

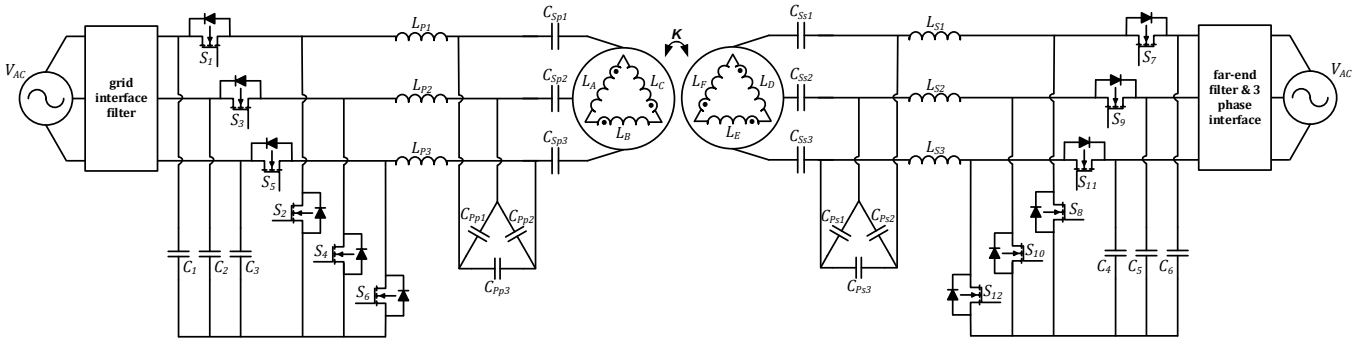

Fig. 2. The proposed ac/ac Oak Ridge Converter topology.

An industrial ESS typically consists of two different connection terminals, ac and dc platforms in the system as demonstrated in Fig. 1 [11]. A bidirectional ac / dc converter is integrated as on-board to the ESSs, converting the ac energy to dc for charging or inverting dc energy to ac grid; in two power flow directions as shown in the figure. An ac/ac WPT system can be integrated between ESSs and grid through coupling coils with a single stage configuration. However, dc platform of WPT requires minimum four power conversion stages as bi-directional; ac/dc (or dc/ac) stage from grid (or to grid), dc/ac (or ac/dc) high frequency inverter (or rectifier), ac/ac through the coupling coils, and ac/dc (or dc/ac) rectifier (or high frequency inverter) stage on the vehicle. Three-phase grid connected power converters are used as a rectifier with power factor correction or inverter for both power flow directions in ac / dc stage that provides unity power factor (PF) and low total harmonic distortion (THD) to the grid. Very few studies on ac/ac converter have been performed for WPT systems. A class-E type ac/ac matrix converter is presented for WPT applications by using field programmable gate array (FPGA) in [12]. Authors in [13] proposed a single-phase ac/ac converter to create high frequency current for CPT systems. However, the input current THD of these systems is very high as shown from the experimental results. It might be convenient to inject the power to the load for a period of time, but the system may not be suitable to run the system continuously; especially in grid connected mode. Additionally, a single stage ac/ac converter is demonstrated for WPT EV charging applications in [14] where the on-board charger on the vehicle side was utilized for vehicle integration with ac output on the WPT system.

In this paper, a novel three-phase Oak Ridge ac/ac converter is proposed for mobile ESSs-grid connectivity application which can be used for grid support or grid ancillary services as well as customer side of the meter benefits. Due to inherent merit of the invented topology, it is possible to convert the three-phase ac grid frequency into high-frequency through three phase coupler coils. The simple unique system ensures less complexity on ac/ac power conversion in WPT applications, reducing the overall system cost. The proposed three-phase converter is driven by phase shifted gate signals between switching legs with 50% duty cycle. Gate signals for negative grid half cycles are inverted versions of the gate signals used for positive grid half cycle. The proposed solution improves the system PF and reduces THD with constant operating frequency and front-end filter considering similar studies. The system's theoretical analysis is provided, and state model is demonstrated in each operating cycle. The system simulation analysis is presented at 10 kW output power with an input of 277 $V_{AC,RMS}$ from three phase ac source and output of 277 $V_{AC,RMS}$. The proposed system input current THD and power factor PF are 3% and 0.99, respectively.

II. The Proposed Oak Ridge Converter and System State Analysis

The proposed three-phase ac/ac converter topology is shown for the WMES in Fig. 2. It comprises a front-end filter, bidirectional three phase active switches, a pair of three phase coupling coils (or a closely coupled three phase transformer in the case of a wired charger) with LCC resonant tuning compensation, and far-end filter and three-phase ac interface to the ESSs. The grid-side frequency and high frequency switching are superimposed through the resonant compensation and coupling coils and fundamental frequency of the energy is transferred to the ESSs side with a 60 Hz sinusoidal carrier signal.

This configuration also provides high frequency isolation between low frequency ac to ac systems that might be used to connect two isolated microgrids or ac systems together. Also, this proposed architecture can be a good alternative to a dual active bridge system that can be used to enable a high frequency isolation through a transformer. This system can also be adaptable to motor drive applications directly connected from the grid.

The three-phase converter state and switch transitions are presented the behavior of the proposed system in Fig. 3 and Fig. 4, respectively. To simplify the circuit analysis, front-end filter,

far-end filter, and three phase interface system losses are assumed to be negligible, bi-directional active switches and gate drive system are ideal and switching losses are not concerned. Also, secondary side active switches are off-state and body diodes are conducting. The proposed circuit system is analyzed in the following operation modes.

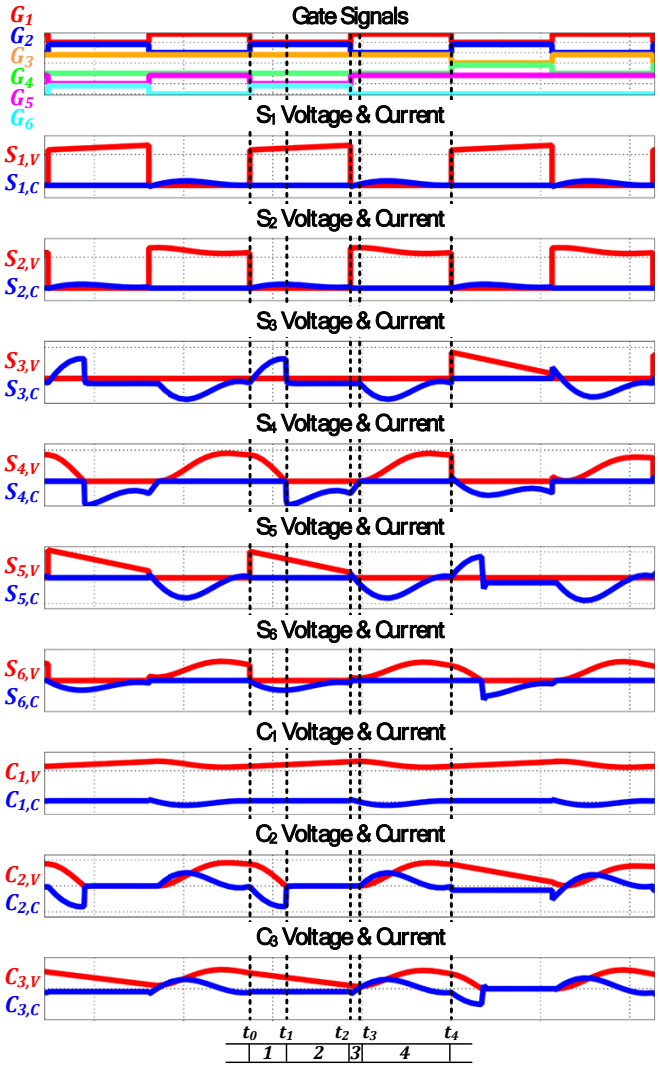

Fig. 3. Three phase voltage and current waveforms of the switches, and decoupling capacitors.

Mode 1 [t_0<t<t_1]

The voltage and current waveforms of the active switches and decoupling capacitors are shown during first interval in Fig. 3. While the phase - A grid voltage is in positive half-cycle and phase - B and phase - C are in negative half-cycle, the active switches S_2, S_3, and S_6 are turned on-state and body diode of switch S_6 is on-state as demonstrated in Fig. 4.a. The coupling capacitors C_1 is charged and C_2, C_3 are discharged to the resonant *LCC* compensation and front-end stage filter and grid interface. The current flows through the second and third phase

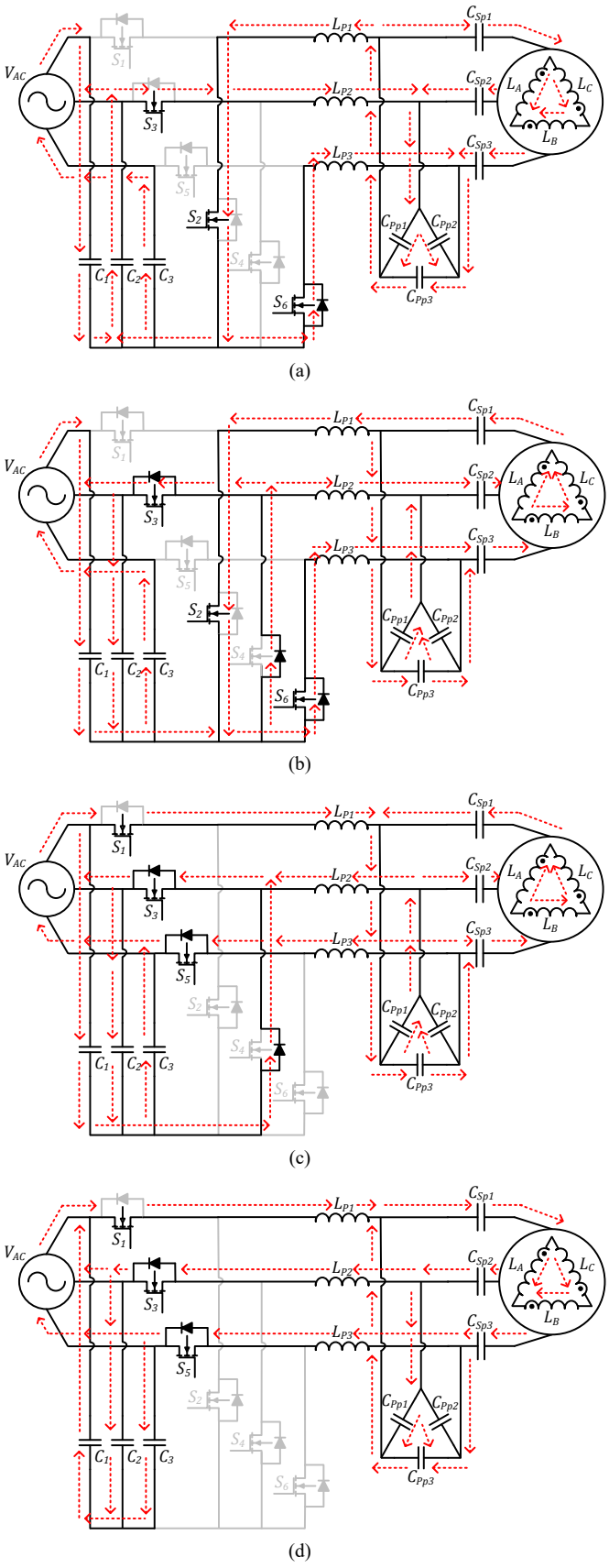

Fig. 4. Mode analysis, current path, and switching transition.

series inductors L_{P2}, L_{P3} and returns from the first phase series inductor L_{P1}. The parallel capacitor between second and third phases C_{Pp2} is charged and C_{Pp1} and C_{Pp3} are discharged through the first phase series inductor L_{P1} and series capacitor C_{Sp1}. In this way, the series capacitor C_{Sp1} is charged through the coupler transformer. The current flows from phase - A winding L_A to the phase - B and phase - C windings L_B, L_C in coupler transformer and series capacitors C_{Sp2}, C_{Sp3} are discharged through the parallel capacitors.

Mode 2 [t_1<t<t_2]

As stated in the second mode in Fig. 3, S_2, S_3, and S_6 are turned on-state and body diodes of switches S_3, S_4, S_6 are on-state. The coupler capacitors C_1 and C_2 are charged and C_3 is discharged thorough front-end filter and grid interface and *LCC* resonant tuning circuit as seen in Fig. 4.b. The current flows through resonant tank series inductors L_{P2}, L_{P3}, and returns from the series inductor L_{P1} and while, the parallel capacitors C_{Pp1} and C_{Pp3} are charged, C_{Pp2} is discharged. The current flows through the series capacitors and charges C_{Sp2} and C_{Sp3} and C_{Sp1} is discharged through the parallel capacitors and series inductor L_{P1}. The current goes through the three-phase coupler transformer phase - B winding L_B and phase - C winding L_C and returns from phase - A winding L_A to the series capacitor C_{Sp1}.

Mode 3 [t_2<t<t_3]

The converter active switches S_1, S_3, and S_5 are on-state, and body diodes of S_3, S_4, and S_5 are conducting in this interval as shown in Fig. 3. Similar to the previous mode, the coupler capacitors C_1 and C_2 are charged and C_3 is discharged. The resonant tank current flows through the first phase series inductor L_{P1} to the parallel capacitors and returns to series inductors L_{P2} and L_{P3}. While the parallel capacitors C_{Pp1} and C_{Pp3} are charged and the parallel capacitor C_{Pp2} is discharged. The series capacitors C_{Sp2} and C_{Sp3} are charged and the first phase series capacitor C_{Sp1} is discharged to the parallel capacitors as demonstrated in Fig. 4.c. The coupler coil current flows through the phase - B winding L_B and phase - C winding L_C and returns from phase - A winding L_A to the series capacitor C_{Sp1}.

Mode 4 [t3<t<t4]

As described in Fig. 3, the converter active switches S_1, S_3, and S_5 are on-state and body diodes of S_3 and S_5 are on-state in this interval. The coupling capacitors C_2 and C_3 are charged and C_1 is discharged to the first phase series inductor L_{P1}. The resonant tank current returns from the second and third phase series inductors L_{P2}, L_{P3} to the coupling capacitors and front-end filter grid interface as presented in Fig. 4.d. The parallel capacitor C_{Pp2} is charged and the parallel capacitors C_{Pp1} and C_{Pp3} are discharged through the first phase series capacitor C_{Sp1}. In this way, the series capacitor C_{Sp1} is charged to the three-phase coupler transformer and the series capacitors C_{Sp2} and C_{Sp3} are discharged to the parallel capacitors and the series inductors L_{P2} and L_{P3}. The coupler coil current flows from phase - A winding L_A and returns to phase - B winding L_B and phase - C winding L_C through the series capacitors C_{Sp2} and C_{Sp3}.

III. THE SYSTEM THEORETICAL ANALYSIS

The proposed CPT system model is considered as a three-phase balanced system with phase-to-phase input voltages v_{ab}, v_{bc}, v_{ca} that can be represented with the maximum values in time domain as,

$$v_{ab}(t) = \sqrt{3}V_{a,max}sin\left(2\pi f_{60}t + \frac{\pi}{6}\right) \quad (1)$$

$$v_{bc}(t) = \sqrt{3}V_{b,max}sin\left(2\pi f_{60}t - \frac{\pi}{2}\right) \quad (2)$$

$$v_{cb}(t) = \sqrt{3}V_{c,max}sin\left(2\pi f_{60}t + \frac{5\pi}{6}\right) \quad (3)$$

where f_{60} is the fundamental frequency of the grid voltage. Furthermore, proposed system can achieve the unity power factor and the input currents i_a, i_b, i_c can be described with their maximum values in time domain as,

$$i_a(t) = I_{a,max}sin(2\pi f_{60}t) \quad (4)$$

$$i_b(t) = I_{b,max}sin\left(2\pi f_{60}t - \frac{2\pi}{3}\right) \quad (5)$$

$$i_c(t) = I_{c,max}sin\left(2\pi f_{60}t + \frac{2\pi}{3}\right) \quad (6)$$

In order to provide the unity power factor at the minimum load condition, the coupling capacitors must be designed at the maximum output power of the system. Power on each phase of the system, p_a, p_b, and p_c can be defined considering the decoupling capacitors' charge and discharge energy within one switching period as,

$$p_a(t) = \frac{1}{2}C_1\left(V_{a,max}sin\left(2\pi f_{60}t + \frac{\pi}{6}\right)\right)^2 f_{sw} \quad (7)$$

$$p_b(t) = \frac{1}{2}C_2\left(V_{b,max}sin\left(2\pi f_{60}t - \frac{\pi}{2}\right)\right)^2 f_{sw} \quad (8)$$

$$p_c(t) = \frac{1}{2}C_3\left(V_{c,max}sin\left(2\pi f_{60}t + \frac{5\pi}{6}\right)\right)^2 f_{sw} \quad (9)$$

where f_{sw} is the operating frequency of the resonant system. Considering the same value of the decoupling capacitors C_d=C_1=C_2=C_3 and the maximum amplitude of the phase voltages V_{pmax}=$V_{a,max}$=$V_{b,max}$=$V_{c,max}$, the total input instantaneous power can be given by sum of the phase input powers as,

$$p_{in}(t) = p_a(t) + p_b(t) + p_c(t) = \frac{1}{2}C_d V_{pmax}^2 \left[sin^2\left(2\pi f_{60}t + \frac{\pi}{6}\right) + sin^2\left(2\pi f_{60}t - \frac{\pi}{2}\right) + sin^2\left(2\pi f_{60}t + \frac{5\pi}{6}\right)\right] f_{sw} \quad (10)$$

The total input instantaneous power is equal to the proposed three-phase balanced system that provides unity input power factor through the wireless coupling coils and resonant

compensation to the output. The input power is obtained by averaging $p_{in}(t)$ over time as,

$$P_{in} = \frac{3}{4} C_d V_{pmax}^2 f_{sw} \tag{11}$$

Since the three-phase output phase voltages are constant at the constant output power and constant input maximum phase voltages V_{pmax}, the decoupling capacitor C_d value can be calculated by the average total output power P_O,

$$C_d = \frac{4P_O}{3V_{pmax}^2 f_{sw} \eta} \tag{12}$$

where η is the proposed converter efficiency. The equivalent circuit of the resonant system is demonstrated in Fig. 5.

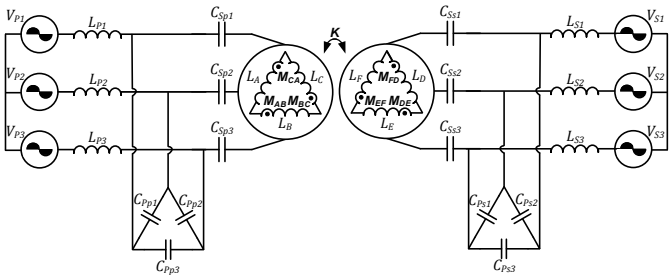

Fig. 5. Equivalent circuit of the proposed converter with mutually coupled Δ / Δ three-phase coupler.

The average value of the equivalent input voltage $V_P=V_{P1}=V_{P2}=V_{P3}$ and the resonant tank phase currents $I_P=I_{P1}=I_{P2}=I_{P3}$ can be written considering the balanced system as,

$$V_P = \frac{1}{\pi} V_{pmax}, \quad I_P = \frac{\pi}{3\eta} \frac{P_O}{V_{pmax}} \tag{13}$$

The equivalent inductance of mutual coupling three phase delta / delta transformer L_P, L_S can be described in matrix form as,

$$L_P = \begin{bmatrix} L_A & M_{AB} & M_{CA} \\ M_{AB} & L_B & M_{BC} \\ M_{CA} & M_{BC} & L_C \end{bmatrix}, \; L_S = \begin{bmatrix} L_D & M_{DE} & M_{FD} \\ M_{DE} & L_E & M_{EF} \\ M_{FD} & M_{EF} & L_F \end{bmatrix} \tag{14}$$

where M_{AB}, M_{BC}, and M_{CA} are the mutual inductance of the transmitter coil between phases L_A and L_B, L_B and L_C, and L_C and L_A, respectively, and M_{DE}, M_{EF}, and M_{FD} are the mutual inductance of the receiver side coil between phases L_D and L_E, L_E and L_F, and L_F and L_D, respectively. The series resonant tuning inductors $L_{Ps}=L_{Ps1}=L_{Ps2}=L_{Ps3}$ can be calculated as,

$$L_{Ps} = \frac{V_{pmax}}{\pi(2\pi f_{sw}) I_P} = \frac{3\eta}{\pi^2 (2\pi f_{sw})} \frac{V_{pmax}^2}{P_O} \tag{15}$$

The delta connected parallel resonant tuning capacitors $C_{Pp}=C_{Pp1}=C_{Pp2}=C_{Pp3}$ and the series connected resonant tuning capacitor values $C_{Ps}=C_{Ps1}=C_{Ps2}=C_{Ps3}$ can be expressed by,

$$C_{Pp} = \frac{1}{3(2\pi f_{sw})^2 L_{Ps}}, \quad C_{Ps} = \frac{1}{(2\pi f_{sw})^2 (L_P/3 - L_{Ps})} \tag{16}$$

The proposed system is symmetrical and transmitter side is identical to the receiver side. Thus, described voltage, current, and component calculation functions can be described similarly as in the receiver.

IV. Simulation Results

The prominent parameters of the simulation are summarized in Table I.

TABLE I - Simulated System Parameters

Symbol	Parameter	Value
$V_{I,AC}$	ac input voltage	277 $V_{AC,RMS}$
$V_{O,AC}$	ac output voltage	277 $V_{AC,RMS}$
P_O	output power	10 kW
L_i	input filter inductor	1.2 mH
C_d	decoupling capacitor	1 µF
L_{Ps}	primary series inductor	4.27 µH
C_{Pp}	primary parallel capacitor	255 nF
C_{Ps}	primary series capacitor	340 nF
L_P	primary self-inductances	42 µH
L_S	secondary self-inductances	42 µH
C_{Ss}	secondary series capacitance	340 nF
C_{Sp}	secondary parallel capacitance	255 nF
L_{Ss}	secondary series inductor	4.27 µH
k	coupling co-efficient	0.15
f_{60}	grid frequency	60 Hz
f_{SW}	operating frequency	88.5 kHz
t_{dead}	dead time	600 ns

The simulation results of the proposed Oak Ridge Converter are presented for a three-phase system at 10 kW, 277 $V_{AC,RMS}$ ac input, and 277 $V_{AC,RMS}$ output voltage as demonstrated in Fig. 6. The three-phase coupler is designed for a coupling factor of 0.15 in the simulation. As seen from the simulation results in Fig. 6 (a) and (b), the input and output current THD is below 3% and PF is around 0.99 for both input and output of the system. The three-phase input voltage and current amplitudes are directly transferred to the receiver side of the system in bidirectional operation by unique converter merit over the grid frequency.

The phase-A resonant tank voltage and current waveforms are given for both input and output resonant tank terminals in Fig. 6 (c). As seen from the figures, the high frequency waveform is superimposed with the grid frequency envelope by the ORC and transferred to the output through the resonant compensation and couplers. The phase angle of the envelope grid frequency is shifted by 70° at the receiver side according to the simulation results. Fig. 6 (d) shows the zoomed-in view of the resonant tank voltages and currents on the primary and secondary sides. The system operates at the resonant frequency with third harmonic injected current waveforms from the primary side. Additionally, receiver side switches are kept OFF

and behave as a rectifier through the freewheeling diodes as seen from the figures.

analysis of the system is presented with the decoupling capacitor and resonant components design equations. Three-phase grid

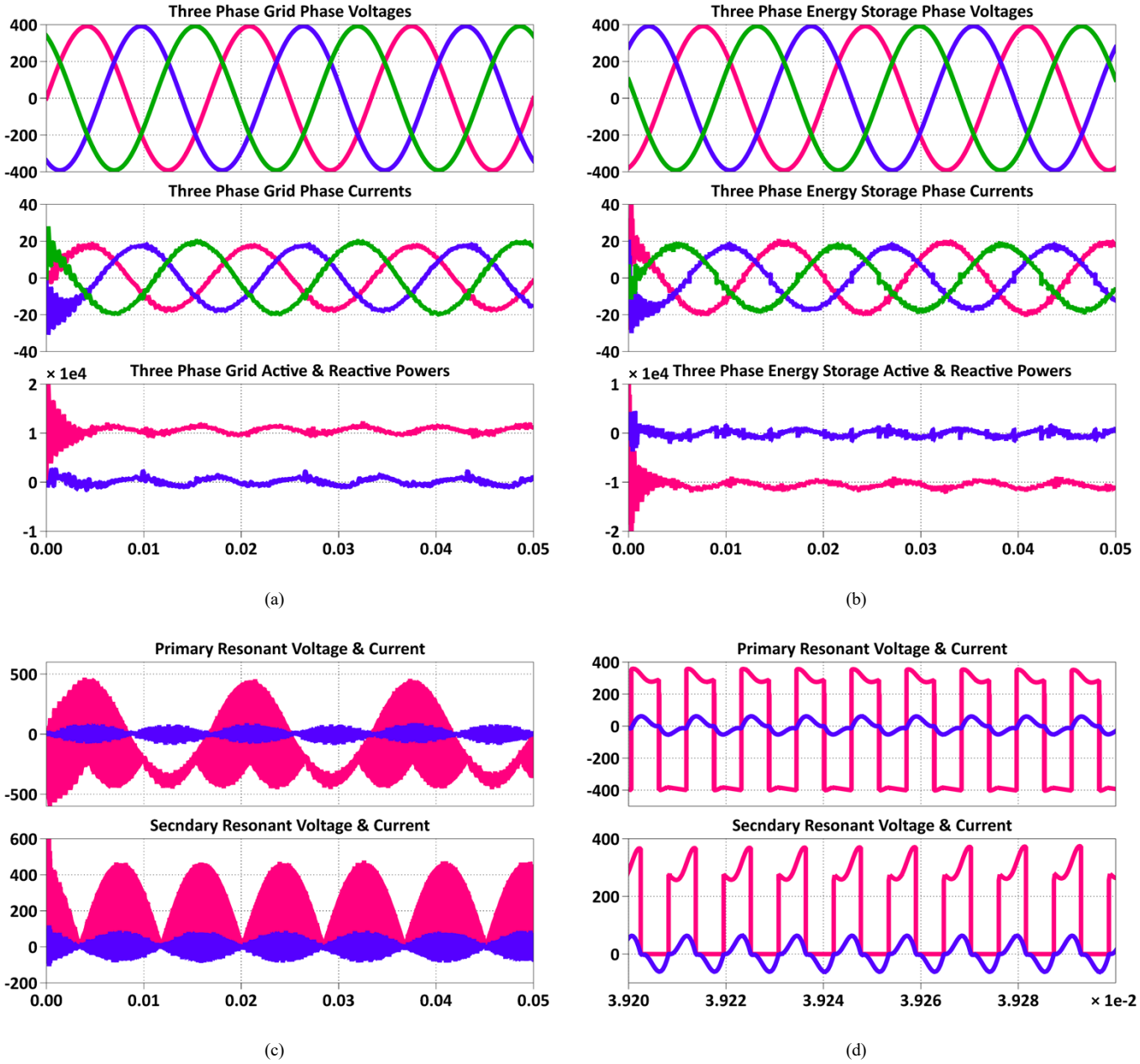

(a) (b)

(c) (d)

Fig. 6. Simulation results of the proposed system with grid to energy storage power flow: (a) grid side three-phase voltages, currents, and active & reactive power, b) energy storage side three-phase voltages, currents, and active & reactive power, c) primary and secondary side resonant tank voltage & current waveforms, d) zoomed-in view of primary and secondary side resonant tank voltage and current waveforms.

V. Conclusions

In this study, a novel Oak Ridge ac/ac converter topology is presented for WMESS systems. The proposed topology can be used for wired or wireless ESSs charging systems by using Oak Ridge Converter that integrates the front-end PFC rectifier with the high-frequency inverter. The state analysis of the proposed idea is described by the switch state conditions, Theoretical

and output voltage and current waveforms are presented with active and reactive powers. The three-phase grid voltage 277 $V_{AC,RMS}$ is transferred to the output with a voltage of 277 $V_{AC,RMS}$ at 10 kW power, 0.99 power factor and 3% current THD. The resonant tank voltage and current waveforms are shown with the hybrid high (88.5 kHz) and envelope grid (60 Hz) frequencies from the primary and secondary sides. It is shown that the three-phase grid system at 60 Hz frequency can

be converted to high-frequency ac voltage by Oak Ridge Converter and transferred through the resonant network and couplers to the energy storage system input ac terminals. With the proposed ORC technology, the front-end PFC rectifier stage can be eliminated while maintaining near unity power factor (0.99) and low total harmonic distortions (3%) which are compliant by the grid power quality standards.

TABLE II

	Conventional Three Phase CPT	Proposed Oak Ridge Converter CPT
	Grid + Filter + Three Phase PFC / Inverter + Three Phase HF DC/AC Inverter + Three Phase Coupler Transformer + Three Phase Rectifier / HF DC/AC Inverter + Battery	Grid + Filter + Oak Ridge Inverter DC/AC + Three Phase Coupler Transformer + Rectifier / Oak Ridge Inverter DC/AC + On-board Energy Storage Charger + Battery
FET	18	12
Inductor PFC	3	0
PFC Ind. & Cap.	2	0
Design Stage	2	1

The comparison of the proposed Oak Ridge Converter with the conventional three-phase system is presented in Table II. As seen from the table, the proposed system can reduce the number of components and as a result, it reduces the weight, volume, and cost of the system while maintaining the same functionality. Moreover, the proposed approach reduces the number of power conversion stages to be designed; therefore, it reduces the time and effort that needs to be dedicated to design and fabrication of the converter. Furthermore, the proposed converter eliminates the phase inductors and bulk dc bus capacitors in the conventional PFC designs.

ACKNOWLEDGEMENTS

This project is funded by Oak Ridge National Laboratory's Laboratory Directed Research and Development (LDRD) Program's Transformational Energy Science and Technology (TEST) initiative with the project ID LOIS-9505. This research used resources available at the Power Electronics and Electric Machinery Research Center located at the National Transportation Research Center, a DOE EERE User Facility operated by the Oak Ridge National Laboratory (ORNL). The authors would like to thank the TEST Initiative Lead, Dr. Ilias Belharouak for his support of this work and his guidance. Authors also acknowledge the support and guidance of ORNL Sustainable Transportation Program Manager, Dr. Rich Davies, which is greatly appreciated.

REFERENCES

[1] N. Anglani, G. Oriti, and M. Colombini, "Optimized energy management system to reduce fuel consumption in remote military microgrids," *IEEE Transactions on Industry Applications*, vol. 53, no. 6, pp. 5777-5785, Nov.-Dec. 2017.

[2] H. H. Abdeltawab and Y. A. I. Mohamed, "Mobile energy storage scheduling and operation in active distribution systems," *IEEE Transactions on Industrial Electronics*, vol. 64, no. 9, pp. 6828-6840, Sep. 2017.

[3] E. Asa, K. Colak, M. Bojarski, D. Czarkowski, "Asymmetrical duty-cycle and phase-shift control of a novel multiport CLL resonant converter," *IEEE Journal of Emerging and Selected Topics in Power Electronics*, vol. 3, no. 4, pp. 1122-1131, Dec. 2015.

[4] K. Colak, E. Asa, M. Bojarski and D. Czarkowski, "Asymmetrical duty-cycle control of a novel multi-port CLL resonant converter," in Proc., *IEEE Applied Power Electronics Conference and Exposition (APEC)*, pp. 3019-3024, March 2015, Charlotte, NC.

[5] B. R. Ravada, N. R. Tummuru, and B. N. L. Ande, "PV-wind and hybrid energy storage integrated multi-source converter configuration based grid-interactive microgrid," *IEEE Transactions on Industrial Electronics*, vol. 68, no. 5, pp. 4004-4013, May 2021.

[6] A. Vettuparambil, K. Chatterjee, and B. G. Fernandes, "A multiport converter interfacing solar photovoltaic modules and energy storage with DC microgrid," *IEEE Transactions on Industrial Electronics*, vol. 68, no. 4, pp. 3113-3123, April 2021.

[7] O. C. Onar, G.-J. Su, E. Asa, J. Pries, V. Galigekere, L. Seiber, C. White, R. Wiles, and J. Wilkins, "20-kW bi-directional wireless power transfer system with energy storage system connectivity," in Proc., *IEEE Applied Power Electronics Conference and Exposition (APEC)*, pp. 3208-3214, March 2020, New Orleans, LA.

[8] E. Asa, K. Colak, and D. Czarkowski, "Analysis of cascaded multi-output-port converter for wireless plug-in Hybrid/On-Board EV chargers," in *Proc., IEEE Applied Power Electronics Conference and Exposition (APEC)*, pp. 1323-1328, March 2016, Long Beach, CA.

[9] K. Colak, E. Asa, D. Czarkowski, and H. Komurcugil, "A novel multi-level bi-directional DC/DC converter for inductive power transfer applications," in *Proc., IEEE Industrial Electronics Society Annual Conference (IECON)*, pp. 3827-3831, November 2015, Yokohama, Japan.

[10] E. Asa, K. Colak, D. Czarkowski, and B. Tamyurek, "Efficiency analysis of a bi-directional DC/DC converter for wireless energy transfer applications," in *Proc., IEEE Energy Conversion Congress and Exposition (ECCE)*, pp. 594-598, Sept. 2015, Montreal, QC.

[11] TMEIC 2.5MW Energy Storage Systems. Available online: https://www.tmeic.com/product/energy-storage

[12] P. S. Huynh, D. Vincent, L. Patnaik, and S. S. Williamson, "FPGA-based PWM implementation of matrix converter in inductive wireless power transfer systems," in *Proc., IEEE PELS Workshop on Emerging Technologies: Wireless Power Transfer (WoW)*, pp. 1-6, June 2018, Montréal, QC, Canada.

[13] H. L. Li, A. P. Hu, and G. A. Covic, "A direct AC–AC converter for inductive power-transfer systems," *IEEE Transactions on Power Electronics*, vol. 27, no. 2, pp. 661-668, Feb. 2012.

[14] E. Asa, J. Pries, V. Galigekere, S. Mukherjee, O. C. Onar, G. J. Su, and B. Ozpineci, "A novel AC to AC wireless power transfer system for EV charging applications," in *Proc., IEEE Applied Power Electronics Conference and Exposition (APEC)*, pp. 1685-1690, March 2020, New Orleans, LA.